Available online at www.sciencedirect.com
SCIENCE DIRECT
Thermochimica Acta 443 (2006) 78–86
thermochimica acta
www.elsevier.com/locate/tca

Measurement and modeling of the glass transition temperatures of multi-component solutions

Binal N. Shah, Constance A. Schall *

Department of Chemical and Environmental Engineering, University of Toledo, 2801 W. Bancroft Street, Toledo, OH 43606, USA

Received 18 August 2005; received in revised form 15 November 2005; accepted 4 January 2006
Available online 8 February 2006

Abstract

Protein crystals are usually grown in multi-component aqueous solutions containing salts, buffers and other additives. To measure the X-ray diffraction data of the crystal, crystals are rapidly lowered to cryogenic temperatures. On flash cooling, ice frequently forms affecting the integrity of the sample. In order to eliminate this effect, substances called cryoprotectants are added to produce a glassy (vitrified) state rather than ice. Heretofore, the quantity of cryoprotectant needed to vitrify the sample has largely been established by trial and error. In this study, differential scanning calorimetry (DSC) was used to measure the melting (T_m), devitrification (T_d) and glass transition (T_g) temperatures of solutions with a range of compositions typical of those used for growing protein crystals, with the addition of glycerol as cryoprotectant. The addition of cryoprotectant raises the T_g and lowers the T_m of bulk solution thereby decreasing the cooling rates required for vitrification of protein crystals. The theoretical T_g value was calculated using the apparent volume fraction using the Miller/Fox equation extended for multi-component systems. The experimental values of T_g were within approximately ±4% of that predicted by the model. Thus, the use of the model holds the promise of a rational method for the theoretical determination of the composition of cryoprotectant requirement of protein crystallization solutions.

Keywords: Glass transition temperature; Multi-component solutions; Cryogenic cooling of protein crystal

1. Introduction

There are limited data for the glass transition temperatures, T_g, of multi-component mixtures and few studies comparing experimental and predicted values of T_g for such mixtures. The studies reported herein were undertaken in an attempt to increase available data for multi-component mixtures and to test the ability of multi-component models to predict glass transition temperatures. Differential scanning calorimetry (DSC) was used to measure the glass transition (T_g), the melting (T_m) and the devitrification (T_d) temperatures of multi-component aqueous mixtures representative of those used in protein crystallization.

Protein crystals and their crystallizing solutions are 'flash cooled' to cryogenic temperatures for X-ray data collection in structure determination experiments. Data collection at cryogenic temperatures is necessary in order to reduce ionizing radiation damage due to X-rays [1–4]. Protein crystals are composed of large volume fractions of water with wide channels (∼10–100 Å in diameter), which are filled with the crystallizing solution. When cooling the protein crystals to low temperatures for X-ray data measurement, ice can form and expand within the solvent channels and surrounding mother liquor. Ice disrupts the protein crystal lattice as well as giving rise to additional Bragg scattering. Most aqueous solutions require the addition of chemicals termed cryoprotectants in order to form glasses at practically attainable cooling rates (water has a reported glass transition temperature between 130 and 140 K [5–10]). Thus, cryoprotectants such as glycerol, D-sorbitol, 1-2-propanediol, dimethyl sulfoxide or cryosalts [11] are used to raise the glass transition temperature and depress the melting point. The cooling rates required for vitrification are then attainable using liquid or gaseous cryogens such as nitrogen or helium.

Cryoprotectants are also often used in lyophilization of biomolecules or food for preservation [12–14]. During lyophilization, water is sublimated causing an increase in the concentration of cryoprotectant and thereby an increase in T_g and a decrease in T_m. As cryoprotectant concentration increases, a concentration at which T_g and T_m are approximately equal (the

* Corresponding author. Tel.: +1 419 530 8097; fax: +1 419 530 8086.
E-mail address: cschall@eng.utoledo.edu (C.A. Schall).

0040-6031/$ – see front matter © 2006 Elsevier B.V. All rights reserved.
doi:10.1016/j.tca.2006.01.003

maximal freeze concentration) is reached. At these high concentrations, ice nucleation cannot occur. It is generally not possible to use these very high concentrations of cryoprotectant for protein crystal cryoprotection for diffraction studies since addition of cryoprotectant often increases protein solubility and leads to dissolution of the crystal. In contrast to lyophilization, flash cooling of protein crystals also requires that no significant water removal occurs during sample vitrification. Water is an integral part of the crystal lattice and with its removal, the protein crystal lattice collapses resulting in loss of Bragg diffraction.

The search for appropriate cryoprotectant composition for protein cryo-crystallography is often a trial and error procedure resulting in the sacrifice of protein crystals for unsuccessful trials. Often the number of available crystals for structural studies is quite limited with crystal growth times of days to months. Structural biological studies would be aided if crystal losses could be minimized in flash cooling trials by having initial attempts close to optimal conditions. However, any rational approach to cryoprotectant selection requires knowledge of the T_g values of protein crystallization solutions.

Hampton crystal screens (Hampton Research) are widely used for crystallization of proteins. These screens consist of multi-component aqueous-based mixtures of buffers, salts, polymers (i.e. polyethylene glycol) and alcohols. These solutions largely represent the solvent in the protein crystal channels and the mother liquor surrounding the crystal.

For cryo-crystallography, crystals are mounted in a thin film of mother liquor held by surface tension in a fiber loop, commonly referred to as a cryoloop [15]. In our earlier studies [16], we determined the amount of glycerol (as cryoprotectant) required to successfully flash cool a selected set of Hampton screen solutions in nominal 1, 0.5 and 0.1 mm cryoloops (Table 1). It was found that the measured glass transition temperatures of cryoprotected solutions for the 1 mm loop fell into a narrow temperature range. Cryoprotection requirement also correlated with sample size, indicating that T_g gives information about the target temperature to be reached in order to avoid ice formation.

Herein, we measured the glass transition of a selected set of Hampton crystal screen/glycerol mixtures and mother liquor–glycerol mixtures used for D-xylose isomerase crystals by DSC. Knowledge of the compositional dependency of T_g for the multi-component solutions used in protein crystallization can allow selection of cryoprotectant based on a set value for T_g.

2. Experimental

2.1. Materials

The set of Hampton crystal screen I (Hampton Research, HR2-110) samples (sample number and composition are listed in Table 1) and solutions used for D-xylose isomerase crystals were mixed with glycerol (Fisher Scientific, G33-500) in 5% (v/v) increments. The D-xylose isomerase solutions were composed of an aqueous solution of 0.1 M Tris(hydroxymethyl) aminomethane buffer (Fisher Scientific, BP 154-1), pH 8.0 with 10 mM $MgCl_2$ (Fisher Scientific, M33-500) and an overall ammonium sulfate (Fisher Scientific, A702-3) concentration of 20% (w/v) in the solution/glycerol mixture. Twenty percent (w/w) ammonium sulfate was found to be immiscible in solutions of 55% (v/v) glycerol or greater. Because of its high viscosity, glycerol was heated to 343 K in a water bath and then pipetted with a positive displacement pipetter into the room temperature solution in 5% (v/v) increments.

Density was calculated by measuring the weight for a known volume (500–1000 μl) of sample (five to six times each sample) on a four-place analytical balance. The average density of the Hampton screens is tabulated in Table 1.

Table 1
Minimum glycerol requirement for vitrification in commercially available cryoloops and measured room temperature density of the selected Hampton screen I samples (screen number is listed as #)

#	Salt	Buffer	Precipitant	Percent glycerol (v/v) to vitrify nominal loop size			Density (g/cm^3) average ± S.D.
				1.0 mm	0.5 mm	0.1 mm	
2	None	None	0.4 M Potassium Na tartrate	35	20	0	1.065 ± 0.002
3	None	None	0.4 M Ammonium dihydrogen phosphate	40	25	–	1.035 ± 0.002
4	None	0.1 M Tris–HCl[a], pH 8.5	2 M Ammonium sulfate	25	10	0	1.145 ± 0.002
6	0.2 M $MgCl_2$	0.1 M Tris–HCl[a], pH 8.5	30% (w/v) PEG 4000	15	5	0	1.071 ± 0.007
7	None	0.1 M Na cacodylate, pH 6.5	1.4 M Na acetate	25	5	0	1.073 ± 0.004
18	0.2 M Mg acetate	0.1 M Na cacodylate, pH 6.5	20% (w/v) PEG 8000	15	10	0	1.069 ± 0.001
25	None	0.1 M Imidazole, pH 6.5	1 M Na acetate	30	10	0	1.050 ± 0.008
32	None	None	2 M Ammonium sulfate	20	10	0	1.140 ± 0.003
34	None	0.1 M Na acetate, pH 4.6	2 M Na formate	25	15	0	1.090 ± 0.005
35	None	0.1 M Na HEPES[b], pH 7.5	0.8 M Na dihydrogen phosphate, 0.8 M K dihydrogen phosphate	25	10	0	1.143 ± 0.003
36	None	0.1 M Tris–HCl[a], pH 8.5	8% (w/v) PEG 8000	40	20	0	1.025 ± 0.004
37	None	0.1 M Na acetate, pH 4.6	8% (w/v) PEG 4000	35	15	0	1.028 ± 0.003

[a] Tris(hydroxymethyl)aminomethane hydrochloride.
[b] 4-(2-Hydroxyethyl)piperazine-1-ethanesulfonic acid sodium salt.

2.2. Equipment and DSC methods

The glass transition temperatures of the mixtures were measured using a Perkin Elmer Pyris 1 power-compensated DSC. The DSC was operated at sub-ambient temperatures, with nitrogen shield gas and high purity helium purge gas (99.995%) to prevent ice formation around the DSC cover and furnace. The Pyris 1 DSC is equipped with a Cryofill liquid nitrogen cooling system to obtain temperatures down to 113 K. The DSC temperature was calibrated using the solid–liquid and solid–solid phase transition of cyclohexane at 279.7 and 186.1 K [17] and of cyclopentane at 179.6 and 138.1 K [18].

The sample (3–10 μl for a detectable signal) was pipetted into a 20 μl aluminum pan, covered and then sealed using a sample pan crimper press. The samples were weighed with a four-place analytical balance. The DSC cooling rate was not rapid enough to produce vitrified samples needed in order to observe a glass transition. Because of this, samples were rapidly cooled by plunging the sealed sample pan in either liquid nitrogen or a solid/liquid nitrogen mixture. Most samples did not consistently vitrify in liquid nitrogen due to the Leidenfrost effect requiring solid/liquid nitrogen. The solid/liquid nitrogen mixture was prepared by evacuating a desiccator containing a Dewar of liquid nitrogen. Nitrogen evaporates under vacuum, leading to a temperature decrease and freezing of nitrogen. Vacuum was released, and the sample was rapidly plunged in the nitrogen solid/liquid mixture. The sample pan was then transferred to the pre-cooled DSC sample holder (113 K).

The cooled sample was held at the initial temperature in the DSC for 10 min and then heated from 113 to 298 K, using a heating rate of 5 K/min. The sample was then held for 5 min at the highest temperature. The glass transition temperature was obtained from the intersection of tangent lines from about 5 K below the change in baseline slope and about 2–3 K after the onset of the slope change (Fig. 1). Least square analysis was applied to the data points 5–10 K below and above the glass transition to obtain the equations for the tangent lines (inset shown in Fig. 1) and the intersection point calculated. The glass transition is often followed by devitrification (exothermic peak) where the sample crystallizes into the thermodynamically stable state. The devitrification temperature was obtained from the intersection of the baseline and the tangent of the exothermic peak and is listed in Tables 2 and 3. At higher temperatures the sample melts, producing a sharp endothermic peak. The melting temperature was determined by analyzing peak onset temperatures and is listed in Tables 2 and 3.

For most of the samples a single measurement was performed for T_g. However, to assess the experimental variability in the reported T_g values, repeated measurements were made for Hampton screen samples 2 and 4 containing 35% (v/v) and 25% (v/v) glycerol, respectively (four repeats for sample 2 and six repeats for sample 4). The standard deviations about the mean value of T_g were 0.5 K for sample 2 and 1.0 K for sample 4. The standard deviations about the mean values of T_d, the devitrification temperature, and T_m, the melting temperature, were 0.7 and 0.9 K for sample 2 and 0.7 and 1.0 K for sample 4, respectively.

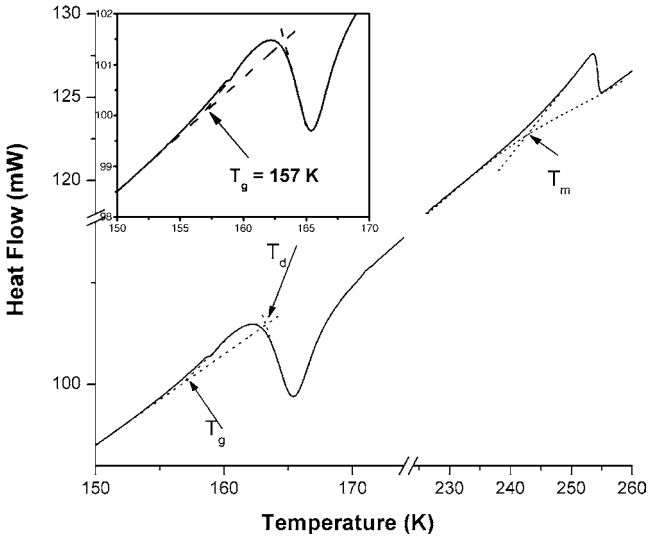

Fig. 1. Analysis of heat flow vs. temperature data to calculate T_g, T_d and T_m for Hampton screen I solution #4, with 25% glycerol (v/v). Endothermic events produce peaks above the baseline and exothermic events produce peaks below the baseline. Glass transition, T_g, is followed by an exothermic devitrification peak, T_d, at about 163.2 K and an endothermic peak, T_m, at 241.4 K. T_g was determined by calculating the intersection of tangent lines of the baseline before and after the slope change of heat flow vs. temperature (see inset).

3. Theory and T_g calculation

There are a number of semi-empirical and theoretically derived models for the compositional dependency of T_g for multi-component systems. The Fox equation [19] is an example of an empirical equation that has been extended for multi-component systems (Eq. (1)). The Fox equation is found to predict glass transition of multi-component plasticizer–polymer mixtures well [20].

$$\frac{1}{T_g} = \frac{w_1}{T_{g_1}} + \frac{w_2}{T_{g_2}} \ldots + \frac{w_n}{T_{g_n}} \tag{1}$$

Miller et al. [21] derived a general relationship between T_g of a non-ideal binary or multi-component solution and its composition. In their derivation, the transition of glass to liquid is qualitatively described as the disintegration of a network of free volume. The free volume in the liquid is viewed as a continuous network of ‘lakes and channels’. As temperature decreases this free volume decreases until it reaches a critical level at T_g where the network disintegrates. Using percolation theory, the authors derived a quantitative relationship between T_g and composition for a multi-component solution:

$$\frac{1}{T_g} = \sum_{i=1}^{n} \frac{\varphi_i}{T_{g_1}} + \frac{1}{0.19} \varphi^E \langle \alpha^E \rangle \tag{2}$$

where φ_i is the apparent volume fraction of component i ($\varphi_i = x_i V_i / V$), x_i the mole fraction of component i, V_i the molar volume of pure component i and V the molar volume of the mixture at the glass transition temperature of the mixture; T_{gi} is the glass transition temperature of pure component i, $\langle \alpha^E \rangle$ the excess thermal expansion coefficient and $\varphi^E = V^E/V$, is the excess volume fraction (V^E is the excess molar volume of the

Table 2
Glass transition (T_g), devitrification (T_d) and melting (T_m) temperatures of Hampton screen I solutions for varying glycerol concentrations

#	Percent glycerol (v/v)	T_g (K)	T_d (K)	T_m (K)
2	35	157.4	170.8	243.5
	40	158.4	166.1	241.3
	60	167.7		
3	35	157.0	163.9	245.1
	40	157.0	167.9	243.3
	45	157.9	172.1	241.3
4	25	156.8	163.2	241.4
	30	157.9	166.0	240.3
	35	159.2	182.1	234.5
	40	163.8	198.1	228.6
	50[a]	161.3		
	60[a]	173.1		
	70[a]	171.8		
	80[a]	180.8		
6	10	157.4	168.1	252.2
	15	157.7	170.5	249.6
	20	158.3	178.7	246.1
7	25	160.2	169.2	247.4
	30	161.0	171.6	243.1
18	15	158.2	167.8	251.4
	20	157.6	168.2	250.6
	25	158.3	172.5	245.8
	30	158.7	181.7	241.0
25	30	157.8	166.5	246.0
	35	159.5	171.1	243.0
32	25	157.1	162.3	243.0
	30	156.9	164.6	238.7
	40	161.1	200.8	218.7
	45[a]	162.1		
	70[a]	178.6		
	80[a]	180.7		
34	25	157.5	166.9	245.0
	30	160.6	168.7	242.7
	40	161.4	191.6	231.2
	45[a]	166.1		
35	25	156.6	168.0	245.9
	30	159.5	169.0	243.9
36	30	152.9	163.2	249.7
	35	156.3	165.6	245.2
	40	159.4	178.7	242.5
	45[a]	159.4	191.9	235.7
	50[a]	163.0		
37	35	156.7	166.0	242.5
	40	158.1	177.5	241.6

[a] Where no data appears for T_d and T_m, devitrification and melting transitions were not observed in DSC data.

mixture). The Fox equation can be derived from Miller's expression for the special case where excess volume can be neglected and the ratios of the pure components to the mixture density are approximately equal at all temperatures (see Appendix A). Miller's equation (Eq. (2)) was used to predict the T_g for mixtures of sodium chloride, trehalose and water (neglecting the excess terms of mixing), providing a reasonable prediction of T_g [21].

Table 3
Glass transition (T_g), devitrification (T_d) and melting (T_m) temperatures of mother liquor used for D-xylose isomerase crystals for varying glycerol concentrations

Percent glycerol (v/v)	T_g (K)	T_d (K)	T_m (K)
30	161.2	169.8	236.1
35	163.6	184.2	233
40	165.8	203.0	228.8
45[b]	168.9		220.7
50[a]	171.1		

[a] Where no data appears for T_d and T_m, devitrification and melting transitions were not observed in DSC data.
[b] T_d was not observed in DSC data for this sample, this may be due to slow relaxation into crystalline state for the DSC to show a signal.

To apply Eq. (2) to a multi-component system, T_g of the pure components must be known in addition to volumetric data as a function of temperature for the pure species and mixture. The last term, containing mixture properties (excess properties) is typically small compared to the other terms and can often be neglected. This allows calculation of mixture T_g with only pure component properties. For a binary system the molar volume of the mixture is given by Eq. (3):

$$V = x_1 V_1 + x_2 V_2 + V^E \tag{3}$$

Neglecting the excess volume term, volumetric data can be used to calculate φ_i for every component at the glass transition temperature. Volumetric data of pure components is often limited, and the temperature dependency of this data can be estimated by linearly extrapolating volumetric data for two different temperatures. Eq. (2) is transformed into an objective function, $F(T)$ and T_g is calculated using $F(T_g) = 0$ [21].

$$F(T) = \frac{1}{T} - \sum_{i=1}^{n} \frac{\varphi_i}{T_{g_1}} \tag{4}$$

If the ratio of density variation with temperature can be assumed to be constant, Eq. (2) can be written as Eq. (5), henceforth known as Miller/Fox equation (see Appendix A).

$$\frac{1}{T_g} = \frac{m_1}{m_t T_{g_1}(\rho_1(T_g)/\rho_t(T_g))} + \frac{m_2}{m_t T_{g_2}(\rho_2(T_g)/\rho_t(T_g))} + \frac{m_3}{m_t T_{g_3}(\rho_3(T_g)/\rho_t(T_g))} + \frac{m_4}{m_t T_{g_4}(\rho_4(T_g)/\rho_t(T_g))} \tag{5}$$

The Fox Eq. (1), Miller's Eq. (2) and the Miller/Fox Eq. (5) were compared to literature values for glycerol–water systems neglecting the excess molar volume of mixing (Fig. 2). All equations require T_g of the pure components. The glass transition temperature of glycerol, measured using DSC, was found to be 186 K in agreement [22–24] or in close agreement with reported values (187 K [25] and 190 K [26,27]). A value of 138 K is used for T_g of water [5]. For volumetric data required for application of Miller equation (Eq. (2)), the density of supercooled water between 239 and 263 K was linearly extrapolated to low temperatures using data by Hare and Sorenson [28]. Variation of molar volume with temperature of glycerol was obtained from

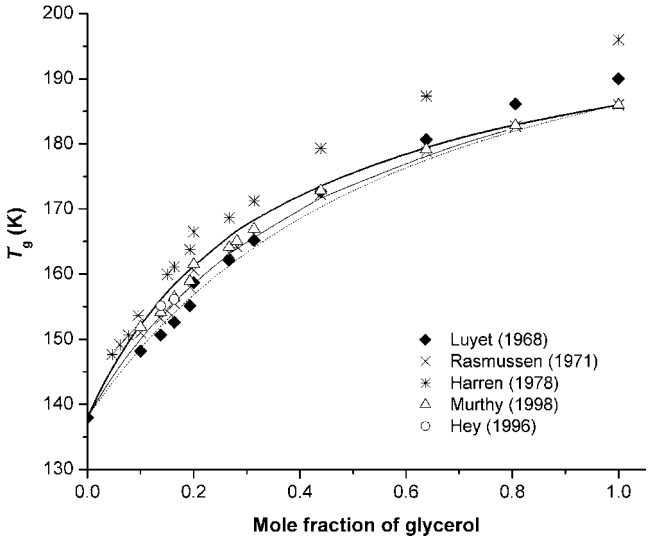

Fig. 2. T_g of glycerol–water solutions with data from various authors. Lines represent the Fox equation (___), Miller/Fox's equation (—) and Miller's equation (- - -).

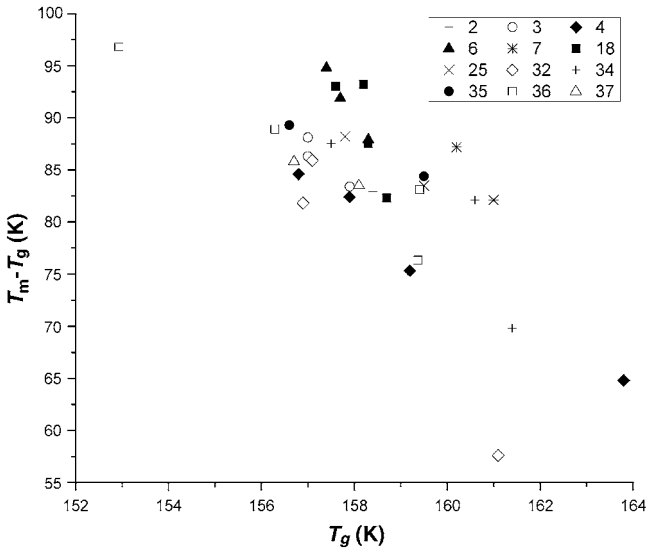

Fig. 3. Variation of $(T_m - T_g)$ as a function of T_g. As cryoprotectant concentration increases, T_g increases and T_m decreases narrowing the temperature range for possible ice nucleation. The Hampton screen # is indicated in the legend box. Compositions of the screens can be found in Table 1.

Huck et al. [29]. Volumetric data for mixture was calculated using Eq. (3).

For the Miller/Fox equation, the ratio of density of glycerol [29] and water [30] was calculated at 10 °C temperature intervals over a temperature range from −30 to 30 °C yielding an average value of 1.0049 and 0.9952 g/cm^3 with a standard deviation of 0.004 and 0.5%, respectively. These ratios were assumed to remain constant down to the glass transition temperature of the mixture, eliminating the necessity of extrapolating volumetric data.

There is a fairly wide deviation in reported T_gs for water–glycerol mixtures as illustrated in Fig. 2. This wide deviation may be due to differences in glycerol source, method of measurement or the heating rate in DSC or DTA studies. T_g of pure glycerol as measured by Luyet and Rasmussen [27] by DTA using the same heating rate of 5 °C/min shows a difference of 4 K. Murthy [22] reported a T_g of 186 K measured at 10 °C/min, whereas Harran [31] reported a T_g of 196 K measured at 20 °C/min using DSC. All the equations (Eqs. (1), (2) and (5)) give reasonable predictions of the reported T_gs although the Miller/Fox equation appears to provide an estimate of T_g, approximately mid-way through the data sets. Eqs. (1), (2) and (5) were used for calculation and comparison of T_g values for Hampton crystal screen I, #4, #34 and #36 solutions to assess their utility for our multi-component solutions.

4. Results and discussion

As the temperature of the sample increases above the glass transition, the molecular mobility increases, often resulting in a crystallization event where components form a more stable state. This transition results in an exothermic peak (Fig. 1). The temperature of this transition is referred to as the devitrification temperature, T_d. On heating to the melting temperature, T_m, an endothermic peak is then observed. For those samples that devitrified, T_d and T_m were determined from the onset of the endothermic and exothermic peaks in the DSC thermograms. The T_g, T_d and T_m of a sampling of screen and D-xylose isomerase solutions with variable amounts of added glycerol are listed in Tables 2 and 3. T_d and T_m were not observed for samples containing greater than 40–45% (v/v) glycerol. In these samples, a direct transition from a glassy to liquid state occurs. This can be attributed to the very high viscosity of these solutions.

In general, as glycerol concentration increases, T_g increases and T_m decreases. Thus, the cryoprotectant glycerol narrows the temperature window for ice formation through these favorable changes in both T_g and T_m. This narrowing of $(T_m - T_g)$ with increasing T_g is more clearly seen graphically in Fig. 3.

Solution composition can be adjusted to raise T_g (and lower T_m) to a target value by addition of cryoprotectant. In order to predict compositional requirements for a selected value of T_g, use of predictive models for T_g such as those outlined in the previous section may be helpful. In order to ascertain the utility of multi-component models in estimating T_g the Fox equation (Eq. (1)), Miller's equation (Eq. (2)) and Miller/Fox's equation (Eq. (5)) were used to calculate T_g for screens #4, #34, #36 solutions with added glycerol.

Eqs. (1), (2) and (5) require T_g of all pure components in the solution. T_g of water and glycerol were available from literature sources as outlined in Section 3. It is not possible to measure the T_g of pure salts, whereas T_m is easily measured by DSC for salts that do not decompose on heating. We were also unable to vitrify pure PEG 4000 and PEG 8000. Hence, a hypothetical estimate of T_g was used for salts and PEG as follows: Kanno [32] derived a constant value of 2/3 for the ratio of T_g/T_m using Lindemann's interpretation of melting [33]. Simha and Boyer [34] derived this same ratio based on a free volume approach for polymer systems. Angell et al. [7], have reported T_g/T_m values for aqueous electrolyte solutions close to this 2/3 value as

Table 4
T_g and T_m used for pure salts

Salt	T_g (K)	T_m (K)	Remarks and reference	Density (g/cc)
Ammonium sulfate	368.8	508	Decomposes at 553.15 K [30]	1.7647[b] [30]
Imidazole	241.8	362.65	[30]	1.0103 [30]
K Na tartrate	232.1	348.15	Reported as decomposition temperature for sodium potassium tartrate tetrahydrate at 348.15 K [30]	1.79 [30]
Magnesium acetate	397.4	596.15	[30]	1.42 [37]
Magnesium chloride	658.1	987.15	[30]	2.325 [30]
Ammonium dihydrogen phosphate, monobasic	308.8	463.15	[30]	1.8 [30]
K dihydrogen phosphate, monobasic	350.5	525.75	[30]	2.34 [30]
Na dihydrogen phosphate, monobasic	248.8	373.15	Decomposes at 373.15 K [30]	1.839[c]
PEG 4000	222.1	333.1	Measured T_m [Hampton Research (HR2 605)]	1.3961[c]
PEG 8000	223.4	335.1	Measured T_m [Hampton Research (HR2 515)]	1.336[c]
Sodium acetate	400.9	601.35	[30]	1.528
Sodium cacodylate	222.1	333.15	Reported as melting point of sodium cacodylate tetrahydrate in [30]	1.25 (assumed)
Sodium formate	353.6	530.45	[30]	1.92 [30]
Na HEPES[b]	339.4	509.15	Decomposes at 509.15 K as measured and reported for HEPES in CRC Handbook [30]	1.2886[c]
Tris(hydroxymethyl) aminomethane	269.6	404.5	Meaured as 406.65 K and reported as [38]	1.2865[c]
Tris hydrochloride[a]	281.43	422.15	Measured T_m, in agreement with value reported at http://www.hamptonresearch.com/support/msds/2579M.pdf	1.2375[c]

[a] Tris(hydroxymethyl) aminomethane hydrochloride.
[b] 4-(2-Hydroxyethyl)piperazine-1-ethanesulfonic acid sodium salt.
[c] Densities measured by displacement with mineral oil as described in Section 4.

have Sakka and Mackenzie [35] for inorganic glasses. Similarly, Murthy and Nayak [36] have reported the values of T_g/T_m for various organic liquids that fall close to 2/3. In application of the Fox and Miller/Fox equations to our data, T_g values of salts and PEG were estimated using the 2/3 ratio for T_g/T_m and the melting points of the pure components as listed in Table 4. The T_m of salts in screen #34 (sodium formate and sodium acetate) were available in the literature [30], whereas the T_m values for PEG 8000 and the buffer salt Tris–HCl used in screen #36 were measured by DSC (after calibration using indium and zinc).

The Miller equation (Eq. (2)) also requires volumetric data for individual components and the mixture as a function of temperature. The excess volume terms were neglected and volumetric data was estimated from that of water and glycerol as outlined for water–glycerol mixtures in Section 3. The molar volumes of PEG 8000 and the salts, sodium formate, sodium acetate and Tris–HCl were held constant at their room temperature values

Table 5
Comparison of T_g predicted with the Fox equation, Miller/Fox equation and Miller equation with experimentally measured T_g for Hampton screen I, solution #4, #34 and #36

#	Percent glycerol (v/v)	Experimental T_g^{exp} (K)	Fox equation T_g^{model} (K)	Miller/Fox equation T_g^{model} (K)	Miller equation T_g^{model} (K)
4	25	156.8	168.2	159.7	158.0
	30	157.9	169.3	161.1	159.4
	35	159.2	170.5	162.6	160.9
	40	161.2	171.6	164.2	162.4
	50	161.3	173.9	167.3	165.6
	60	171.0	176.3	170.7	169.1
	70	171.8	178.7	174.2	172.9
	80	180.8	181.1	177.9	176.9
34	25	157.5	158.9	152.7	151.3
	30	160.6	160.6	154.5	153.0
	40	161.4	164.0	158.2	156.5
	45	166.1	165.7	160.1	158.4
36	30	152.9	155.6	152.8	151.2
	35	156.3	157.6	154.7	153.0
	40	159.4	159.7	156.7	154.9
	45	159.4	161.8	158.8	156.9
	50	163.0	163.9	160.9	158.9

The Fox equation and Miller/Fox equation yield a closer approximation of T_g over the measured range of glycerol concentration compared to the Miller equation.

Table 6
Deviation of T_g values from experimental values

#	Percent glycerol (v/v)	Experimental T_g^{exp} (K)	Fox equation T_g^{model} (K)	Percent difference[a]	Miller/Fox equation T_g^{model} (K)	Percent difference[a]
2	35	157.4	156.5	0.5	153.2	2.7
	40	158.4	158.6	−0.2	155.2	2.0
	60	167.0	167.3	−0.2	164.1	1.7
3	35	157.0	156.0	0.6	152.8	2.7
	40	157.0	158.2	−0.8	154.9	1.3
	45	157.9	160.4	−1.6	157.0	0.6
4	25	156.8	168.2	−7.3	159.7	−1.8
	30	157.9	169.3	−7.2	161.1	−2.0
	35	159.2	170.5	−7.1	162.6	−2.1
	40	161.2	171.6	−6.5	164.2	−1.8
	50	161.3	173.9	−7.8	167.3	−3.6
	60	171.0	176.3	−3.1	170.7	0.2
	70	171.8	178.7	−4.0	174.2	−1.4
	80	180.8	181.1	−0.2	177.9	1.6
6	10	157.4	160.9	−2.2	155.4	1.3
	15	157.7	162.3	−2.9	156.8	0.6
	20	158.3	163.6	−3.4	158.3	0.0
7	25	160.2	157.9	1.4	153.6	4.1
	30	161.0	159.7	0.8	155.3	3.5
18	15	158.2	157.2	0.6	153.3	3.1
	20	157.6	158.8	−0.8	154.8	1.8
	25	158.3	160.4	−1.3	156.4	1.2
	30	158.7	162.1	−2.1	158.1	0.4
25	30	157.8	157.2	0.4	151.2	4.2
	35	159.5	159.1	0.3	153.1	4.0
32	25	157.1	167.2	−6.5	158.8	−1.1
	30	156.9	168.4	−7.3	160.3	−2.2
	40	161.1	170.8	−6.1	163.4	−1.5
	45	162.1	172.1	−6.2	165.1	−1.8
	70	178.6	178.3	0.2	173.8	2.7
	80	180.7	180.8	−0.1	177.6	1.7
34	25	157.5	158.4	−0.6	152.7	3.0
	30	160.6	160.1	0.3	154.5	3.8
	40	161.4	163.6	−1.4	158.2	2.0
	45	166.1	165.4	0.4	160.1	3.6
35	25	156.6	162.0	−3.4	154.8	1.1
	30	159.5	163.4	−2.5	156.5	1.9
36	30	152.9	155.6	−1.7	152.8	0.1
	35	156.3	157.6	−0.9	154.7	1.0
	40	159.4	159.7	−0.2	156.7	1.7
	45	159.4	161.8	−1.5	158.8	0.4
	50	163.0	163.9	−0.6	160.9	1.3
37	35	156.7	157.3	−0.4	154.3	1.5
	40	158.1	159.4	−0.8	156.3	1.1

[a] Percent difference defined as $((T_g^{exp} - T_g^{model})/T_g^{exp}) \times 100$.

Table 7
Deviation from experimental value for cryoprotectant solutions for D-xylose isomerase crystals

Percent glycerol (v/v)	Experimental T_g^{exp} (K)	Model (Fox) T_g^{model} (K)	Difference (K) $T_g^{exp} - T_g^{model}$ Fox	Percent difference[a]	Model (Miller/Fox) T_g^{model} (K)	Difference (K) $T_g^{exp} - T_g^{model}$ (Miller/Fox)	Percent difference[a]
30	161.2	170.7	−9.5	−5.9	162.0	−0.8	−0.5
35	163.6	173.1	−9.5	−5.8	164.4	−0.8	−0.5
40	165.8	175.5	−9.7	−5.9	166.8	−1.0	−0.6
45	168.9	176.9	−8.0	−4.7	168.5	0.4	0.3
50	171.1	180.3	−9.2	−5.4	171.9	−0.8	−0.5

[a] Percent difference defined as $((T_g^{exp} - T_g^{model})/T_g^{exp}) \times 100$.

of 5988.0, 35.42, 56.61 and 126.87 cm^3/mol, respectively. The densities of Tris–HCl and PEG 8000 were experimentally determined by measuring displacement of a known weight of their powder with a known volume of light mineral oil. The accuracy of this method of measurement was assessed by measuring the density of ammonium sulfate as 1.7647 g/cm^3, which is very close to the reported value 1.77 g/cm^3 [30].

For the Miller/Fox equation (Eq. (5)), the ratio of pure component and mixture densities were calculated at room temperature and the volume changes of mixing were assumed to be negligible. It was further assumed that the ratio of densities was constant with temperature.

The predicted values of T_g using Eqs. (1), (2) and (5) were compared to the experimentally measured T_g values for screen #4, #34, #36 (Table 5). The Fox equation produced T_g values that more closely approximated the experimentally determined T_gs than did Miller's equation. The Fox equation predicted T_g values within 3 K of the experimentally measured T_gs for screens #34 and 36 and in general predicted higher T_gs than the experimental values. The T_g predicted by Fox equation for #4, #32 and D-xylose isomerase solutions deviated from actual T_g by up to ~11 K for some mixtures. This is largely due to the very high salt concentration (~12–18% (w/w)) in screen 4 solutions containing less than 50% (v/v) glycerol. Both the Fox (Eq. (1)) and the Miller/Fox (Eq. (5)) equations estimated T_gs closer to the experimental values than did the Miller equation. The Miller equation predicted T_gs that were in general 2–8 K lower than measured values. The magnitude of deviations from the actual T_g may be due in part to errors in our estimate of the volumetric properties of pure components and mixture data and elimination of the excess volume term in our application of Miller's equation. On average the Miller/Fox equation estimated T_g values within 3 K of measured values for screens 4 and 36, whereas T_g values were within 3–6 K of measured values for #34.

Since the Miller/Fox equations yielded reasonable estimates of T_g for Hampton screen #4, #34 and #36, T_g of the remaining Hampton screens and D-xylose isomerase crystallization solutions (high weight fraction of salt ~18%) were calculated using this model (Tables 6 and 7). Due to its simple form, the Fox equation was also used to estimate T_g of the remaining solutions. The T_g for salts and PEG were estimated from T_m as described previously. However, the salts ammonium sulfate, potassium sodium tartrate, sodium dihydrogen phosphate, and sodium HEPES decompose upon heating making measurement of T_m for these salts by DSC impossible. The decomposition temperature was used as an estimate of T_m in these cases. Density of the remaining salts for the screen solutions were obtained from the literature (Table 4) or measured as described for Tris–HCl and PEG.

The T_g values obtained from the Fox and Miller/Fox equations are compared with the experimental values in Tables 6 and 7. The percent difference between experimental and calculated T_gs (calculated from the ratio of experimental minus model values to the experimental values) were less than ±4.2% or 6.6 K for the Miller/Fox equation and less than ±12.6% or 12.6 K for the Fox equation. In general, the Fox equation and the Miller equation both performed well with low salt (less than ~12 wt%) solutions and solutions with PEG. For higher salt solutions, particularly those containing a high weight fraction of ammonium sulfate (screens 4, 32 and the xylose isomerase solutions), the Miller/Fox equation produced much better estimates than the Fox equation. For other screens with 12 wt% salt or greater (#35 with sodium and potassium dihydrogen phosphate) or high PEG (#6 with 30% (w/v) PEG 4000), the Miller/Fox equation again produced better estimates than the Fox equation.

5. Conclusions

The T_g of multi-component mixtures of water, glycerol, salts and PEG can be estimated using the relatively simple Fox model (Eq. (5)) for low salt solutions (less than ~12 wt%) or the Miller/Fox equation for higher weight fractions of salt. The Fox equation allows calculation of T_g as a function of the weight fraction and T_g values of the pure components. For the Miller/Fox equation T_g is calculated as a function of apparent volume fraction and requires the densities of pure components at a reference temperature (i.e. room temperature). Glass transition temperatures for components such as salts that do not easily form glasses, can be estimated from the more experimentally accessible melting temperature by assuming the ratio T_g/T_m is equal to 2/3. For those compounds that decompose upon heating, the decomposition temperature can be used in place of the melting temperature in calculation of T_g.

Comparison of experimental data with model predictions demonstrates utility of this approach in estimating of T_g for cryoprotected protein crystallization solutions. Components of a solution with T_gs significantly above that of water will afford cryoprotection. These components can include buffers and salts. Use of the Fox and Miller/Fox equations allow formulation of cryoprotected solutions using a variety of chemical constituents.

Acknowledgements

This research was sponsored by the National Aeronautics and Space Administration grant NAG8-1838. The authors are thankful to Dr. Jeffrey Dunn, Dr. B. Leif Hanson and Unmesh Chinte for their helpful suggestions.

Appendix A

Neglecting excess properties, Eq. (2) for a quaternary mixture can be written as, where T_g is a function of volume fraction and pure component glass transition temperature only:

$$\frac{1}{T_g} = \frac{\varphi_1}{T_{g_1}} + \frac{\varphi_2}{T_{g_2}} + \frac{\varphi_3}{T_{g_3}} + \frac{\varphi_4}{T_{g_4}}$$

Substituting for φ_i,

$$\frac{1}{T_g} = \frac{x_1 V_1}{V T_{g_1}} + \frac{x_2 V_2}{V T_{g_2}} + \frac{x_3 V_3}{V T_{g_3}} + \frac{x_4 V_4}{V T_{g_4}}$$

Substituting,

$$x_i = \frac{n_i}{n_t}; \quad V_i = \frac{v_i}{n_i}; \quad V = \frac{v_t}{n_t}$$

where n_i is moles of component i, n_t total moles in the mixture, v_i volume of component i and v_t the total volume of the mixture.

$$\frac{1}{T_g} = \frac{v_1}{v_t T_{g_1}} + \frac{v_2}{v_t T_{g_2}} + \frac{v_3}{v_t T_{g_3}} + \frac{v_4}{v_t T_{g_4}}$$

Substituting,

$$v_i = \frac{m_i}{\rho_i}; \quad v_t = \frac{m_t}{\rho_t}$$

where, m_i is mass of component i and ρ_i density of pure component i; m_t is the total mass of mixture and ρ_t the density of the mixture.

$$\frac{1}{T_g} = \frac{m_1}{m_t T_{g_1}(\rho_1(T_g)/\rho_t(T_g))} + \frac{m_2}{m_t T_{g_2}(\rho_2(T_g)/\rho_t(T_g))} + \frac{m_3}{m_t T_{g_3}(\rho_3(T_g)/\rho_t(T_g))} + \frac{m_4}{m_t T_{g_4}(\rho_4(T_g)/\rho_t(T_g))}$$

Assuming that density of all components and the mixture are approximately equal at all temperatures, the above equation takes the form of the Fox [19] equation extended for multi-component systems

$$\frac{1}{T_g} = \frac{w_1}{T_{g_1}} + \frac{w_2}{T_{g_2}} + \frac{w_3}{T_{g_3}} + \frac{w_4}{T_{g_4}} \quad \text{(A.1)}$$

References

[1] E.F. Garman, T.R. Schneider, Macromolecular crystallography, J. Appl. Cryst. 30 (1997) 211–237.
[2] E. Garman, Cool data: quantity and quality, Acta Cryst. D55 (1999) 1641–1653.
[3] H. Hope, Cryocrystallography of biological macromolecules: a generally applicable method, Acta Cryst. B44 (1988) 22–26.
[4] D.W. Rodgers, Cryocrystallography, Structure 2 (12) (1994) 1135–1140.
[5] J.A. McMillan, S.C. Los, Vitreous ice: irreversible transformations during warm-up, Nature 206 (1965) 806–807.
[6] M. Sugisaki, S. Hiroshi, S. Syuzo, Calorimetric study of the glassy state IV. Heat capacities of glassy water and cubic ice, Bull. Chem. Soc. Jpn. 41 (1968) 2591–2599.
[7] C.A. Angell, E.J. Sare, Glass-forming composition regions and glass transition temperatures for aqueous electrolyte solutions, J. Chem. Phys. 52 (3) (1970) 1058–1068.
[8] G.P. Johari, On the heat capacity, entropy and 'glass transition' of vitreous ice, Philos. Mag. 35 (4) (1977) 1077–1090.
[9] O. Mishima, H.E. Stanley, The relationship between liquid, supercooled and glassy water, Nature 396 (1998) 329–335.
[10] A. Hallbrucker, E. Mayer, G.P. Johari, Glass–liquid transition and the enthalpy of devitrification of annealed vapor-deposited amorphous solid water. A comparison with hyperquenched glassy water, J. Phys. Chem. 93 (1989) 4986–4990.
[11] K.A. Rubinson, et al., Cryosalts: suppression of ice formation in macromolecular crystallography, Acta Crystallogr., Sect D: Biol. Crystallogr. 56 (2000) 996–1001.
[12] R.G. Harrison (Ed.), Protein Purification Process Engineering: Bioprocess Technology, vol. 18, Marcel Dekker Inc, New York, 1994, p. 317.
[13] F. Franks, Freeze-drying of bioproducts: putting principles into practice, Eur. J. Pharm. Biopharm. 45 (1998) 221–229.
[14] B.J. Fuller, Cryoprotectants: the essential antifreezes to protect life in the frozen state, Cryo-Letters 25 (6) (2004) 275–388.
[15] T.-Y. Teng, Mounting of crystals for macromolecular crystallography in a free-standing thin film, J. Appl. Cryst. 23 (1990) 387–391.
[16] U. Chinte, et al., Sample-size: an important parameter in flash cooling macromolecular crystallization solutions, J. Appl. Cryst. 38 (3) (2005) 412–419.
[17] J.G. Aston, G.J. Szasz, H.L. Fink, The heat capacity and entropy, heats of transition, fusion and vaporization and the vapor pressures of cyclohexane. The vibrational frequencies of alicyclic ring systems, J. Am. Chem. Soc. 65 (1943) 1135–1139.
[18] J.G. Aston, H.L. Fink, S.C. Schumann, The heat capacity and entropy, heats of transition, fusion and vaporization and the vapor pressures of cyclopentane. Evidence for a nonplanar structure, J. Am. Chem. Soc. 65 (1943) 341–346.
[19] T.G. Fox, Influence of diluent and copolymer composition on the glass temperature of a polymer system, Bull. Am. Phys. Soc 2 (1) (1956) 123.
[20] M.M. Feldstein, G.A. Shandryuk, N.A. Plate, Relation of glass transition temperature to the hydrogen-bonding degree and energy in poly (*N*-vinyl pyrrolidone) blends with hydroxyl-containing plasticizers. Part 1. Effects of hydroxyl group number in plasticizer molecule, Polymer 42 (2001) 971–979.
[21] D.P. Miller, J.J. de Pablo, H. Corti, Thermophysical properties of trehalose and its concentrated aqueous solutions, Pharm. Res. 14 (5) (1997) 578–590.
[22] S.S.N. Murthy, Some insights into the physical basis of the cryoprotective action of dimethyl sulfoxide and ethylene glycol, Cryobiology 36 (1998) 84–96.
[23] D.H. Rasmussen, A.P. MacKenzie, The glass transition in amorphous water application of the measurements to problems arising in cryobiology, J. Phys. Chem. 75 (7) (1971) 967–973.
[24] M.R. Carpenter, D.B. Davies, A.J. Matheson, Measurement of the glass-transition temperature of simple liquids, J. Chem. Phys. 46 (7) (1967) 2451–2454.
[25] J.A. McMillan, Kinetics of glass transformation by thermal analysis I. Glycerol, J. Chem. Phys. 42 (10) (1965) 3497–3501.
[26] R. Calemczuk, E. Bonjour, Calorimetric study of the relaxation of amorphous glycerol below T_g, Journees de Calorimetrie et d'Analyse Thermique 8 (2) (1977) 13–17.
[27] B. Luyet, D. Rasmussen, Study by differential thermal analysis of the temperatures of instability of rapidly cooled solutions of glycerol, ethylene glycol, sucrose and glucose, Biodynamica 10 (211) (1968) 167–191.
[28] D.E. Hare, C.M. Sorensen, The density of supercooled water. II. Bulk samples cooled to the homogenous nucleation limit, J. Chem. Phys. 87 (1987) 4840–4845.
[29] J. Huck, J. Dufour, A. Bondeau. Density of supercooled glycerol-water solutions, in: Proceedings of the Ninth International Conference on Conduction and Breakdown in Dielectric Liquids, 1987, Salford, Engl.: IEEE, New York, NY, USA.
[30] D.R. Lide (Ed.), CRC Handbook of Chemistry and Physics: A Ready Reference book of Chemical and Physical Data, 84th ed., CRC Press, Boca Raton, 2004–2005.
[31] D. Harran, Thermal behavior and glass transition curve of glycerol–water binary mixtures, Bulletin de la Societe Chimique de France 1–2 (1) (1978) 40–44.
[32] H. Kanno, A simple derivation of the empirical rule $T_g/T_m = 2/3$, J. Non-Cryst. Solids 44 (1981) 409–413.
[33] F.A. Lindemann, The calculation of molecular vibration frequencies, Phys. Chem. 11 (1910) 609–612.
[34] R. Simha, R.F. Boyer, On a general relation involving the glass temperature and coefficients of expansion of polymers, J. Chem. Phys. 37 (1962) 1003–1007.
[35] S. Sakka, J.D. Mackenzie, Relation between apparent glass transition temperature and liquidus temperature for inorganic glasses, J. Non-Cryst. Solids 6 (1971) 145–162.
[36] S.S.N. Murthy, S.K. Nayak, Novel differential scanning calorimetric studies of supercooled liquids, J. Chem. Soc. Faraday Trans. 89 (3) (1993) 509–514.
[37] R.H. Perry, D.W. Green (Eds.), Perry's Chemical Engineers' Handbook, 7th ed., McGraw-Hill, New York, 1997.
[38] S. Durovic, V. Kupcik, Crystallographic data on tris(hydroxymethyl)-aminomethane, Chemicke Zvesti 13 (1959) 565–571.